AIAA Regional Student Conferences
, Multiple Locations
2023 Regional Student Conferences

10.2514/6.2023-71109

Design and Evaluation of a Small-Scale Hybrid Rocket Test Stand

Tanner C. Price[1] and Christopher J. Rathman[2]
Oklahoma State University, Stillwater, OK, 74078, USA

Kurt Rouser[3]
Oklahoma State University, Stillwater, OK, 74078, USA

This paper presents the design, construction, and evaluation of a small, portable hybrid rocket test stand that can accommodate up to a 76-mm diameter engine casing. The primary goal of this study is to determine the most effective and efficient way to build a hybrid rocket test stand for fundamental research purposes, while managing the interface between a high pressure Nitrous Oxide (NOS) system and a solid fuel grain. Various ideas were considered during the design process, including the use of roller bearings and a vertically oriented test stand. The final design of the stand is oriented horizontally with the use of 3 flat aluminum plates mounted to linear bearings on T-slot structural framing. The linear bearings allow the most forward aluminum plate to contact and press against the load cell while maintaining minimal friction with the T-slot structural framing. The oxidizer delivery system begins at a 10-lb NOS bottle at 775-psi, going through a high-pressure steel braided hose, an adjustable pressure regulator, through an on/off solenoid valve, and finally through an orifice plate before being injected into the solid fuel grain. The test stand uses a Futek LLB400 button load cell with capacity of 500-lb, to measure the thrust produced by the engine. A LabVIEW Virtual Instrument controls the opening and closing of the solenoid valve, the ignition process, and thrust measurement. Thrust and specific impulse evaluations of the hybrid rocket engine were conducted on a 38-mm diameter solid fuel grain over various mass flow rates controlled by the pressure regulator, orifice plate area, and nozzle throat area. All solid fuel grains were composed of 3D printed Polylactic Acid and had a typical Bates grain geometry with a core size of 0.65-in, length of 3.5-in, and 50% infill percentage. The constructed test stand resolved differences in thrust and specific impulse; showing the design of the test stand is viable for future research purposes. Additionally, tests show with a feed pressure of 200-psi and an orifice plate hole diameter of 0.234-in, a nozzle diameter of 16/64-in provides the best performance in terms of average and peak thrust, as well as specific and total impulse.

I. Nomenclature

A	=	area
A_e	=	nozzle exit area
C^*	=	characteristic velocity
F	=	force
F_{avg}	=	average force
F_{ext}	=	external force
g_c	=	gravitational unit conversion factor
I_{sp}	=	specific impulse
I	=	total impulse

[1] Graduate Research Assistant, Mechanical & Aerospace Engineering, AIAA Student Member 908386.
[2] Undergrad Research Assistant, Mechanical & Aerospace Engineering, AIAA Student Member 1069182.
[3] Assistant Professor, Mechanical & Aerospace Engineering, AIAA Associate Fellow.

$\dot{m}$ = total mass flow rate
$\hat{n}$ = unit outward normal vector
P_a = atmospheric pressure
P_e = nozzle exit pressure
t_b = burn time
$\vec{V}$ = velocity vector
V_e = nozzle exit velocity
$\forall$ = volume
P = density

II. Introduction

Hybrid rocket engine research and development is necessary in order to close the performance gap of solid and liquid rockets, because hybrid rocket engines traditionally have a lower thrust-to-weight ratio and specific impulse respectively. Chemical propulsion systems are the most well understood and used rocket propulsion systems among the major categories. Within this category there are three types: solid, hybrid and liquid rocket engines. Since the 1930's the focus of chemical propulsion systems has been on solid and liquid rockets, but a newfound interest in hybrid rockets has taken hold. This interest is in part due to a hybrid rocket being chosen to power the second stage of the Tier One, the winner of the $10 million dollar Ansari XPRIZE, as well as advancements in manufacturing technology. Hybrid rockets decrease the concerns around propellant handling, are easy to throttle up or down, and have a potential for a higher specific impulse when compared to solid rocket motors. When compared to liquid engines, hybrid engines tend to have reduced mechanical intricacy, have the ability to contain solid metal additives, and have denser fuels. However, hybrid rocket engines traditionally have poorer performance when compared to solid and liquid rockets in terms of previously mentioned performance parameters. Therefore, this study aims at closing the gap and increasing hybrid engine performance.

Hybrid rocket engines are a type of rocket propulsion system that uses propellant in two states of matter. Typically, one being solid and the other is either liquid or gaseous. The basic concept of a hybrid rocket engine consists of a pressure vessel containing the fluid propellant (oxidizer), and the solid propellant (fuel) placed in the combustion chamber separated by a controlling valve. Closing the gap on solid and liquid rockets necessitates a well-designed, accurate, portable, and novel test stand. Which can accommodate variations in fuel and oxidizer types as well as changes to the size of the overall combustion chamber. The hybrid rocket engines develop for this study involve high-pressure Nitrous Oxide (NOS) flowing from a 10-lb bottle, through a steel braided hose, an adjustable pressure regulator, on/off solenoid valve, an orifice plate, and finally being injected into the combustion chamber. The combustion chamber is comprised of a 38-mm diameter, 7-in long aluminum casing. Inside the combustion chamber is a 3.5-in long fuel grain with a 0.65-in core comprised of 3D printed Polylactic Acid (PLA) at 50% infill.

III. Background & Theory

A. Theory

Rocket engines generally share a consistent set of key performance parameters which are thrust (F), specific impulse (I_{sp}), chamber pressure (P_c), burn time (t_b), characteristic velocity (C*), and burn rate (r_b) [1]. Referring to Newton's second law of motion in Eq. (1), and assuming a one dimensional and steady flow field along with observing there are no influx properties, the momentum equation can be simplified and ideally described as the sum of momentum and pressure forces exiting the control volume through Eq. (3), using the expression for mass flow rate defined in Eq. (2).

$$\frac{1}{g_c} * \frac{\partial}{\partial t} * \iiint \vec{V}\rho d\forall + \frac{1}{g_c} * \iint \vec{V}\rho\left(\vec{V} * \hat{n}\right)dA = \Sigma\overrightarrow{F_{ext}} \tag{1}$$

$$\dot{m} = \frac{g * P_c * A_t}{C^*} \tag{2}$$

$$F = \frac{\dot{m} * V_e}{g_c} + (P_e - P_a) * A_e \tag{3}$$

Specific impulse is a measure of a rocket's thrust per unit of propellant gas weight-flow exiting the nozzle. In the case of hybrid rocket engines, this can also be described as the ratio of total impulse to propellant mass consumed throughout the duration of its burn. The equation for specific impulse can be observed in Eq. (4).

$$I_{sp} = \frac{F}{\dot{w}} \tag{4}$$

Characteristic velocity varies based on the propellant composition, as expressed in Eq. (5), and is used to get a sense for the amount of energy available.

$$C^* = \frac{P_c * A_t}{\dot{m}} = \sqrt{(R_u * T_c)/(\gamma * MW)} * [\frac{2}{\gamma} + 1]^{-\frac{\gamma+1}{2*(\gamma-1)}} \tag{5}$$

A rocket engine's burn rate is a function of chamber pressure and a set of empirical constants known as the burn rate coefficient (a) and burn rate exponent (n) as shown in Eq. (6). An engine's burn rate coefficient and exponent can be determined experimentally and is unique for each propellant composition. It is important to note that burn rate is not unitless and actually has Imperial units of $in*psi^n*s^{-1}$, or $cm*MPa^n*s^{-1}$ for SI units.

$$r_b = a * P_c^n \tag{6}$$

The chamber pressure within the aluminum casing is a key parameter of interest because it determines how fast the solid fuel grain will burn. Chamber pressure is also important for safety purposes. Engine casings must be built with the intent of being able to contain the forces being exerted onto the casing from gases being burned and accelerated through the nozzle. Assuming a fixed nozzle geometry, nearly constant pressure across the length of the solid fuel grain, and that mass flow through the nozzle varies minimally across the engine's burn time $\dot{m}_{in}=\dot{m}_{out}$, instantaneous chamber pressure can be solved as shown in Eq. (7).

$$P_c = [\frac{a*\rho_p*A_b*C^*}{g*A_t}]^{\frac{1}{1-n}} \tag{7}$$

From this, the combination of fluid and solid propellant formulation will hold burn rate coefficient, burn rate exponent, propellant density, and characteristic velocity constant, leaving the profile of the engine's chamber pressure across its burn time to mirror the instantaneous total burning surface area.

Finally, total impulse is measured through taking the integral of thrust produced over the burn time of the rocket motor and is used to quantify the total amount of energy exerted by propellant. Simplification of this integral can be done if either thrust or specific impulse is assumed to be constant as shown in Eq. (8).

$$I = \int F * dt = F * t_b = I_{sp} * m_p \tag{8}$$

B. Background

1. *Hybrid Engine Pros and Cons*

Hybrid rocket engines have several advantages and disadvantages compared to other types of rocket engines like simplicity, low cost, safety, reliability, performance, and efficiency. Because the fuel and oxidizer are mixed in the combustion chamber, the engine can achieve high combustion efficiency and generate high specific impulse which are important for rocket propulsion [2].

There are several disadvantages to using hybrid rocket engines which include: limited by the properties of the solid fuel, difficult to control and modify, relatively low thrust-to-weight-ratio, and limited data and experience. This can make it difficult to predict their performance and reliability. These disadvantages can limit their potential applications and make them less suitable for certain missions or requirements [3].

2. *Hybrid Engine Composition*

There are many considerations when it comes to oxidizers for hybrid rockets: performance characteristics, storability, cost, stability, and ease of use. The oxidizers considered for this study were liquid O_2 (LOX), N_2O (NOS), and H_2O_2 (Hydrogen Peroxide). Liquid oxygen is a widely used cryogenic oxidizer in the space launch industry; it is relatively safe and delivers high performance at a relatively low cost. Hydrogen Peroxide is similar to LOX in its requirements for handling and fire safety; however, it requires less mechanical intricacy than LOX within the rocket [4]. NOS has gained interest recently as a potential oxidizer for hybrid rocket engines. It is non-toxic, has a long shelf

life, a good density, high vapor pressure, the ability to self-pressurize and good overall combustion characteristics. Many hybrid rocket demonstrations in recent years have taken advantage of the self-pressurizing ability of NOS including: SpaceShipOne and SpaceShipTwo, HEROS 3, the rocket test sled trials of Muroran Institute of Technology, TiSpace, and finally the sounding rockets of Space Forest Ltd. NOS is also easy to obtain and store, making it a preferable oxidizer for this study.

When looking at hybrid rocket solid fuels there are many choices that can be made. Fuels can be made of ingredients that have to be cured or created on a 3D printer. Traditionally, the fuel choice for hybrid rocket engines has been any solid hydrocarbon material. This leads to the common use of HTPB [5]. HTPB must be mixed from its liquid components, degassed in a vacuum, then casted and cured in a fuel grain mold. However, some issues with these types of solid fuel grains is the labor-intensive manufacturing process and the limited geometry for internal combustion ports. Another issue with the cast and cure method can be the inconsistency of the mixture. With the advent of additive manufacturing, more specifically, fused deposition modeling (FDM) 3D printers opened the door to more complex port geometries, less labor-intensive manufacturing processes, and various other parameters like infill percentage, internal print structure, layering techniques, and a wide range of materials.

There are many types of filaments on the market today that can be used for 3D printing like PLA, Acrylonitrile Butadiene Styrene (ABS), and Polyethylene Terephthalate Glycol (PETG), as well as some non-plastic materials. The structural, thermal, and mechanical properties of some of these materials are included in the following table.

Table 1 Material Properties of PLA, ABS, and PETG

Material	Structure	P ($g*m^{-3}$)	Tensile Yield Strength (MPa)	Printing Temperature (°C)
PLA	Moderate degree of crystallinity	1225	63	190-220
ABS	Non-crystalline	1010	55	220-260
PETG	Moderate degree of crystallinity	1230	50	230-250

ABS has several mechanical properties that make it attractive as a hybrid rocket fuel. One of the big advantages of ABS is the structural modulus and tensile yield strength [6]. PETG has excellent mechanical properties, but would not be a great hybrid rocket fuel grain. The most intriguing of these filaments is PLA. PLA is relatively similar to ABS in its mechanical properties; however, the biggest advantage it has over ABS is the limited toxicity it produces when combusted. PLA is an incredibly cheap filament to purchase and is considered the most widely available filament. The desired hybrid rocket fuel grain material for this study is PLA.

C. Previous Works

Even though the study of hybrid rockets has been limited until recently, there are some studies focused on hybrid rocket test stand design as well as certain studies focusing on ways in which some performance parameters could be improved. Thomas et. al. designed a lab-scale hybrid rocket test stand using HTPB as their fuel and gaseous oxygen (GOX) as their oxidizer. The design of the stand included the use of structural t-slot aluminum and the use of two linear bearings [7]. The main issue with this test stand design is immobility. Bouziane et. al. also designed a lab scale hybrid rocket test stand, but this study used NOS as the oxidizer and paraffin wax as a fuel grain. The stand was designed to produce 1-kN (225-lb) of thrust and is controlled by a LabVIEW VI. The test stand proved effective [8]; however, the design of this stand does not allow for other sizes of combustion chambers or fuel grains. Another study focusing on hybrid rocket test stand development was done by Summers [9]. This stand design is portable, but once again does not allow for various sizes of combustion chambers or length of the fuel grain. Finally, Utley et. al. designed a portable, flexible use solid rocket test stand. The design was successful in that the stand was able to collect data on specific impulse and total impulse within 1% of the commercially purchased solid rocket motor's manufacturers provided specifications [10].

The predominant nature of studies concerning hybrid rocket engine test stands have been focused on traditional types of fuel, like HTPB, and these test stands only allow for a singular sized combustion chamber. There is a lack of research into the design of a test stand which allows for various sizes of fuel grains, and various types of fuel grains, as well as a lack of research in the mass flow rate of the hybrid rocket engine. With hybrid rocket engines coming to the front of the rocket industry, it seems fitting that a test stand be developed which can be easily adapted or modified

to fit various oxidizers, fuel grains, and casing sizes. Thus, the purpose of this study is to evaluate the design and construction of a portable, adaptable, and lab-scale hybrid rocket test stand.

IV. Test Stand Design

A. Structural Design

The main objective of this study is to design and evaluate a hybrid rocket test stand. The designed test stand for this study attempts to implement the best qualities of some previous works while also including novel parts to enhance the performance of the overall stand and engine.

The base of the test stand is a rectangular steel table. The table has dimensions of 36-in wide, 48-in deep excluding the handle, and 42-in tall including the caster wheels. The table has 4 swivel casters with wheel locks, which allows the test stand to be mobile if desired. The SOLIDWORKS design of the test stand can be seen in Figure 1.

Fig. 1 Test Stand Table

Many of the test stand designs discussed in the third chapter, were able to accommodate a single engine casing size, or a single engine casing length. When beginning the design process, it was of high importance to be able to change the casing size and casing length with ease. This single design parameter was the driving factor in all preliminary designs. The range of casing diameters was defined to be 1.5-in, 2-in, and 3-in; whereas, the range of casing lengths were 5-in to 20-in.

One idea was to mimic the design of Freeman [11], who compresses the motor casing using roller bearings which allows the casing to move forward but not jostle around during testing. While this design seemed enticing, there is a problem when it comes to hybrid rocket engines as the forward closure presses against the load cell. In a hybrid rocket engine, there should be minimal to no loading on the oxidizer feed system, but if this design were to be used the thrust would be directed through the injector fitting.

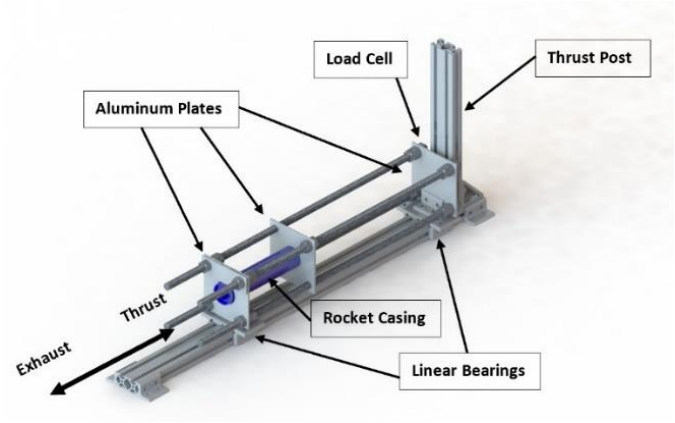

Fig. 2 Test Stand Structure

The final design choice implements the use of the thrust ring on the outer surface of the casing. The casing is inserted into an aluminum plate with a hole large enough to fit the casing, but not large enough to allow the thrust ring through. This plate is connected to two other aluminum plates: one supports the forward end of the casting, and the other presses against the load cell. All three plates are connected with the use of four 1/2-20 threaded rods, and secured with the appropriately sized hex nuts. The most forward and aft plates are connected to a T-slotted framing structural L bracket which are then mounted to T-slot linear bearings. The final design is shown in the figure on the left.

The base of the design is the use of 1-in double T-slot aluminum framing. The vertical thrust post, which braces against thrust force created by the engine, is supported by an open extended gusset bracket opposite the thrust load. The front side of the thrust post contains the Futek LLB400 500-lb capacity load cell. The load cell is connected to a 1/8-in thick aluminum adapter plate. The adapter plate is then bolted to the thrust post and can be moved up or down depending on the size of the engine.

The final main component of the test stand is the thrust ring holder. The thrust ring holder and the aft most aluminum plate hold the thrust ring in place, not allowing any movement of the engine casing. The thrust ring holder is 4-in by 1 1/4-in by 1/8-in and made of aluminum. It, like the 4-in by 4-in aluminum plates is placed on the 1/2-in threaded rods and tightened to hold it in place during testing.

B. Oxidizer Delivery System Design

An oxidizer delivery system was designed to safely introduce the oxidizer to the solid fuel grain and maximize the performance of the engine. The delivery system includes the small 10-lb testing bottle, fittings, steel braided hoses, a pressure regulator, solenoid valve, orifice plate, and forward closure (injector).

The small 10-lb has a 6-Army Navy (AN) male fitting. In order to get the NOS from the bottle, mounted under the top of the table, into the combustion chamber a 6-ft stainless steel braided hose was purchased. This hose can withstand up to 1200-psi and is extremely durable.

The next step in the design process was to determine how to regulate the mass flow rate of oxidizer entering into the combustion chamber. This is done by varying the feed pressure using a pressure regulator and using a single orifice plate. The pressure regulator for this system would be required to handle a supply pressure of at least 1000-psi and have an outlet pressure minimum of 200-psi. Thus, the Pressure Pro II was purchased.

For this mass flow rate regulation setup to work, an orifice plate was also needed. The plate purchased is 6-in by 6-in by 1/4-in and made of 304 Stainless Steel. Because the plate is not threaded, two high pressure pipe flanges and adapters made of 304 Stainless Steel were purchased. The pipe flanges have a thread of 1/2-NPT whereas the rest of the oxidizer delivery system is made up of mostly 1/4-NPT, therefore the 1/4-NPT to 1/2-NPT reducers were needed.

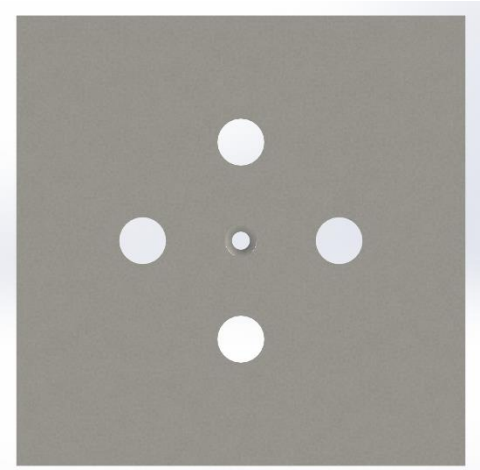

Fig. 3 Orifice Plate Front View

The orifice plate in this feed system is meant to choke the flow. In order for this to occur an extensive analysis was done to determine the diameter of the orifice in the plate.

The first step in the analysis was to make an arbitrary guess as to what the orifice plate hole diameter should be. This was initially chosen to be 1/4-in. The next step would be to find the mass flow rate at various pressures supplied from the pressure regulator. The relation used for this analysis is the Mass Flow Parameter.

$$MFP = (\dot{m} * \sqrt{T_t})/(A * P_t) \tag{9}$$

In order to solve for mass flow rate, equation 9 is rearranged for mass flow rate. Where T_t is the ambient temperature in Rankine and was assumed to be 532 R, P_t is varied from 200-psi to 400-psi by increments of 50-psi, A is the area of the hole in the plate, and MFP is found by using the Gas Tables program in the free AEDsys software. Once this information is input to the Gas Tables, the output MFP is equal to 0.655-(lbm-$R^{1/2}$)/(s-lbf).

After this iterative analysis was complete, the hole diameter of the orifice plate could then be fine-tuned. It was determined the hole diameter should be 0.234-in. The final step in the design process of the orifice plate was to determine how much the hole in the orifice plate should be tapered. If the orifice plate was not tapered, the discharge coefficient would be very low. The discharge coefficient is a function of the ratio of orifice diameter to pipe diameter, β, and the Reynolds Number. By finding the Reynolds Number the discharge coefficient was found to be 0.975 with a tapering angle of 45°. The final design of the orifice plate can be seen in the following Figure 3.

C. Measurement Systems Design

The measurement system is split into the user interface, a measurement input, and

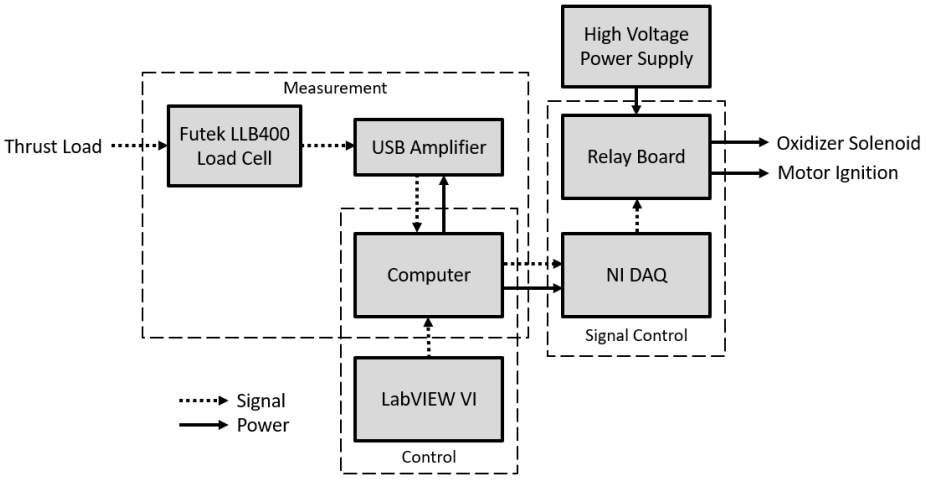

Fig. 4 Measurement System Power and Signal Path

two control outputs. A diagram of how the three groups are connected is below.

A LabVIEW VI was developed to integrate the Futek loadcell, solenoid flow control, and ignition system into a single user interface. This was done using a Message Queue Handling architecture, which allows for parallel processes to take place in independent loops and inherently modular code. The control loops are connected to an event handling loop, where the user interface sends commands. An image of the data collections module can be seen below.

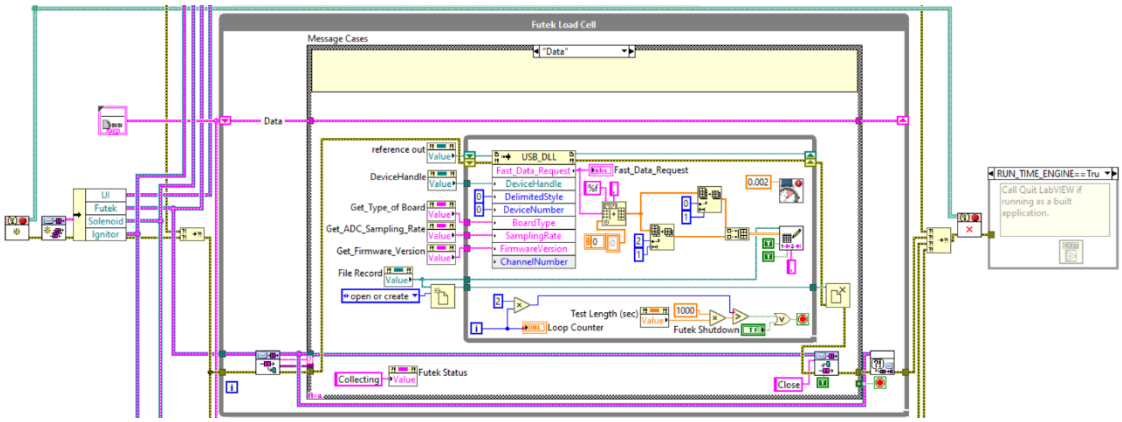

Fig. 5 LabVIEW Data Collection Module

The Futek LLB400 allows for high resolution data collection, which can be configured for each test. For system controls, a National Instruments USB-6211 DAQ board is used for two signal outputs. These two signals go to two high-voltage power relays on an eight-relay board. When pulled high, these relays complete the 24-volt circuit for either the oxidizer solenoid or motor ignition respectively. The duration and timing offsets of these events are inputs with the LabVIEW user interface. The Futek load cell and NI DAQ are both powered from USB 5-volt power and the high-voltage systems are powered by a National Instruments PS-15 Power Supply.

V. Experimental Setup and Procedures

A. Solid Propellant Manufacturing

As mentioned previously, the solid fuel grain is composed of 3D printed PLA. The PLA used for this study is the White Build Series PLA 1.75 mm from MatterHackers. Before the fuel grains could be printed, they needed to be designed using SOLIDWORKS. As mentioned before, the port geometry of the fuel grain is a Bates grain. Initial designs for the fuel grain were 38 mm in diameter, had a length of 3.5 inches, and a port geometry size of 0.65-in.

Although this core geometry works for solid rocket motors, a straight hole through the center of the hybrid grain makes ignition and the combustion process difficult. This is due to the fact that the NOS begins to flow before the ignition process begins. Preliminary tests showed difficulty keeping the igniter in the combustion chamber while the NOS was flowing. Thus, design changes were necessary. All of the initial dimensions stayed the same; however, an igniter holder was added into the final design. The igniter holder itself acts as a "bucket" with a small hole in the bottom to allow the wire leads to come out of the engine and attach to their proper alligator clips. The slicing software, Cura, was used to prepare the design for the 3D printer. Once the solid fuel grains have been designed, sliced, and printed, the grains need to be prepared for testing. Each grain is inserted into a phenolic liner. The phenolic liner is then cut to size, and a solid fuel fit check is completed. The fit check consists of assembling the aluminum casing and snap ring configuration. After the fit check is complete the outer surface of the solid fuel grain is coated in high strength glue and is inserted back into the liner. Once the glue has dried the solid fuel assembly can be fully prepared for testing.

B. Fluid Oxidizer Manufacturing

For ease of mobility as well as being able to attach a NOS bottle to the test stand a small 10-lb testing bottle was purchased. Although, this smaller bottle is sized properly for the test stand, the ability to transfer the NOS from the large 50-lb bottle to the smaller 10-lb bottle became an issue. Therefore, a pump station was needed. This pump fed system comes with all necessary fittings, hoses, and scales to complete a proper fill.. After the small 10-lb testing

bottle has been refilled, it can be mounted to the test stand and connected to the oxidizer delivery system. This is done by threading the hose onto the bottle and ensuring all fittings are tightened throughout the delivery system. When each fitting is properly tightened, the rest of the oxidizer delivery system is prepared. This preparation includes: setting the pressure regulator to the desired outlet pressure, ensuring the solenoid valve is in the off position, the orifice valve bolts are tightened, and the male injector fitting must have fresh thread tape applied.

C. Test Procedures

The electrical systems are powered on and the Futek loadcell and NI DAQ being plugged into the laptop. The alligator clips are tested for voltage. Once confirmed that the alligator clips are not energized, the inserted ignitor is attached. The oxidizer bottle's main valve is then turned open. At the remote laptop station, the LabVIEW VI is started and the loadcell serial number and sampling rate are entered and configured. A save file path is entered. The test duration, oxidizer delay, oxidizer duration, and ignitor delay values are entered. Once the status indicator reads "Configured," the "Start Test" button can be pressed. This will start data logging and run through the oxidizer and ignitor actuations. In a nominal test, the program status indicator will read "Test Ended" once the user configured test duration has surpassed. If an anomaly occurs, the user will press the "Kill System" button, which stops the test and de-energizes the relays. The LabVIEW VI can now be closed, and the collected data can be processed. The test stand can be approached and the combustion chamber carefully removed. The user interface can be seen below.

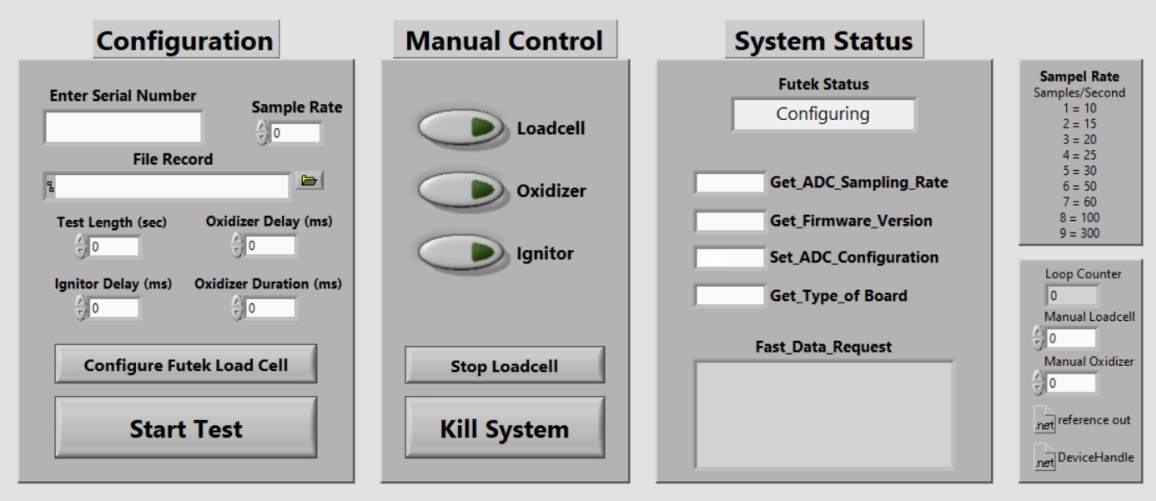

Fig. 6 LabVIEW VI User Interface

VI. Results

After the engine tests, each engine data file was reduced by converting the output thrust data to pound-force and trimming the time to the duration of motor firing. From the reduced data files, peak thrust was found, then average thrust was calculated for each test. Those values were then used, along with the calculated mass flow rate to calculate total impulse and specific impulse. Mass flow rate is calculated by adding the oxidizer and solid fuel mass flow rates. Table 2 below shows the performance values for each engine at a feed pressure of 200-psi and an orifice plate hole size of 0.234-in.

Table 2 Hybrid Rocket Engine Performance Measures

Engine Number	Nozzle Size (#/64)	Peak Thrust (lbf)	Average Thrust (lbf)	Total Impulse (lbf-s)	Specific Impulse (s)
1	13	7.34	3.40	13.84	13.72
2	16	11.38	8.73	34.56	35.19
3	19	9.06	6.88	26.28	27.74
4	25	4.29	1.10	4.49	4.42

Prior to testing, it was hypothesized that a “goldilocks zone” nozzle size would be found where all performance parameters were maximized at a single nozzle size for the given feed pressure and orifice plate hole size. Table 2 helps to prove this hypothesis. During testing engine 1, with the #13 nozzle, showed high levels of visible and audible combustion instability due to the nozzle restricting the mass flow rate and therefore increasing the chamber pressure. This led to limited performance values across the board. Engine 2, with the #16 nozzle, had increased performance in all parameters analyzed for this study. While engine 2 also had some combustion instabilities, it was much less pronounced than engine 1. Engine 3, with the #19 nozzle, showed a slight increase in performance when compared to engine 1, but a decrease in performance when compared to engine 2. Engine 4, with the #25 nozzle, had the worst performance of any engine in this study because the nozzle throat area was too wide, not allowing pressure to build up in the chamber and produce quality combustion. When viewing the solid fuel grains after testing, the grain for engine 4 showed minimal losses in structure from the test. After all testing was complete, the hypothesis was once again looked at when compared to the data. It can be seen from Table 2 that there is indeed a “goldilocks zone” at a nozzle size of 16/64-in. This engine had the best performance because it did not raise the pressure to an unsustainable level inside the combustion chamber, and it was able to hold in enough pressure for combustion.
Figure 7 shows the time-resolved thrust curve for each of the four engine tests on the same plot. Although this is a hybrid rocket engine, the thrust curve for each test has a similar shape to that of a Bates grain solid rocket motor.

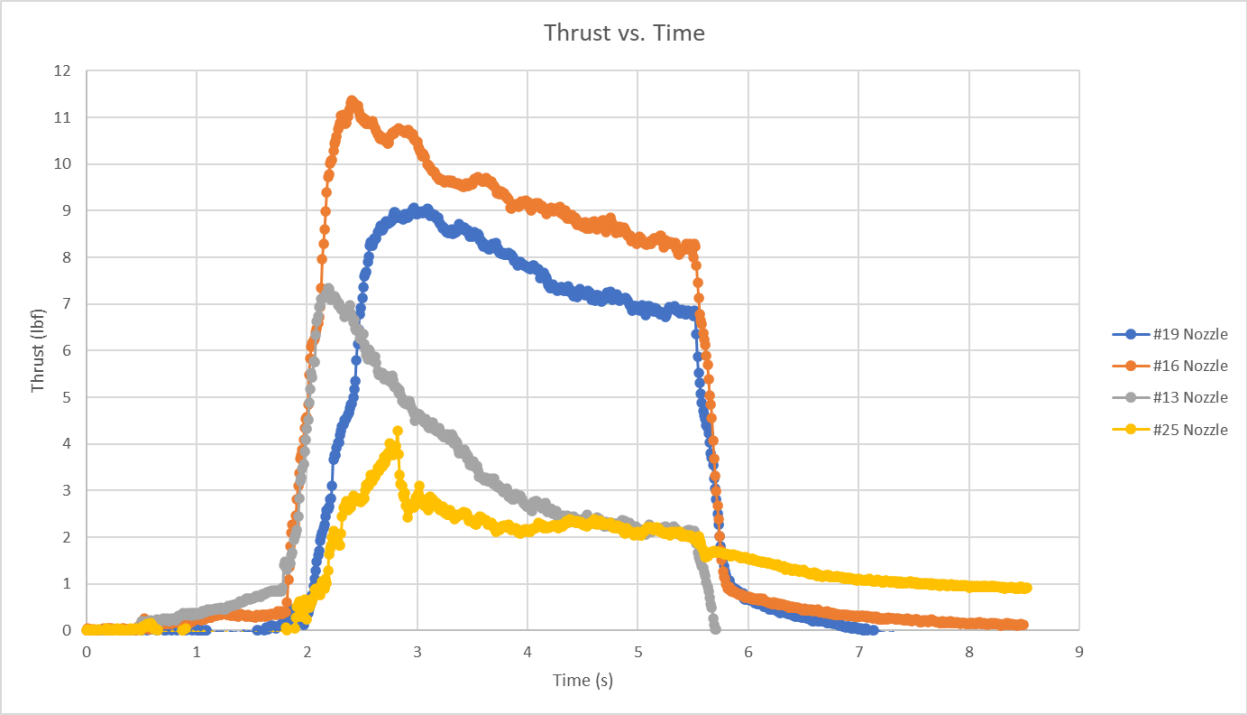

Fig. 7 Thrust Curves for Hybrid Rocket Engine Tests

It is interesting to note that although the tests covered a variety of nozzle throat sizes, each motor came up to its peak thrust within the first 2 to 3 seconds of the test and then trailed off from there. The #19 and #25 nozzles have a later peak thrust time due to the combustion chamber having to build up pressure before combustion can begin. It is obvious that the #16 nozzle in this specific composition and operating parameters provides the highest performance. These results suggest that engine design and operating parameters can have a significant impact on the performance of hybrid rocket engines. Further research may be needed to optimize the design and operating parameters of hybrid rocket engines to achieve even better performance.

VII. Conclusions

The thrust stand design, rationale, and evaluation presented in this paper demonstrate a versatile hybrid rocket engine test stand with the capability to support testing by a variety of groups. The evaluation, which showed the thrust stand to be effective at measuring time-resolved thrust, is representative of the type of university and industry testing that the stand could be used for. It is recommended that further evaluation of the thrust stand take place.

Future testing should include a larger sample size of hybrid rocket engines to better address uncertainty. Future testing should also be done with varying feed pressures, orifice plate diameters, core geometries, infill percentages, infill geometries, fuel and oxidizer composition as well as varying sizes and thrust levels to evaluate the stand with different configurations. It is also recommended that further analysis take place to evaluate the structural limitations of the thrust stand.

Acknowledgments

Tanner Price and Chris Rathman would like to thank Dr. Kurt Rouser and Zac Bycko for their contributions and guidance throughout this study.

References

[1] Heister, S. S., Anderson, J. D., Pourpoint, M. L., & Cassady, G. R., *Rocket Propulsion*, Cambridge Aerospace Series, Cambridge, England, UK, 2019.

[2] Davydenko, N. A., Gollender, R. G., Gubertov, A. M., Mironov, V. V., Volkov, N. N., "Hybrid Rocket Engines: The Benefits and Prospects," *Aerospace Science and Technology*, Vol. 11, No. 1, 2007, pp. 55-60. https://doi.org/10/1016/j.ast.2006.08.008

[3] Mishra, D.P., *Fundamentals of Rocket Propulsion*, 1st ed., CRC Press, Boca Raton, 2017.

[4] Ventura, M. C., and Heister, S. D., "Hydrogen Peroxide as an Alternate Oxidizer for a Hybrid Rocket Booster," *AIAA Journal of Propulsion and Power*, Vol. 11, No. 3, pp. 562-565. https://doi.org/10.2514/3.23878

[5] Sutton, George P., Biblarz, Oscar, *Rocket Propulsion Elements*, 9th ed. Wiley, Hoboken, New Jersey, 2017.

[6] Whitmore, Stephen A., Peterson, Zachary W., Eilers, Shannon D., "Comparing Hydroxyl Terminated Polybutadiene and Acrylonitrile Butadiene Sytrene as Hybrid Rocket Fuels," *AIAA Journal of Propulsion and Power*, Vol. 29, No. 3. https://doi.org/10.2514/1.B34382

[7] Thomas, James C., Stahl, Jacob M., Morrow, Gordon R., Petersen, Eric L., "Design of a Lab-Scale Hybrid Rocket Test Stand," *AIAA 2016-4965. 52nd AIAA/SAE/ASEE Joint Propulsion Conference.* July 2016. https://doi.org/10.2514/6.2016-4965

[8] Bouziane, Mohammed, Bertoldi, Artur Elias De Morais, Milova, Praskovia, Hendrick, Patrick, Lefebvre, Michel, "Development and Testing of a Lab-Scale Test-Bench for Hybrid Rocket Engines," *AIAA 2018-2722. 2018 SpaceOps Conference.* May 2018. https://doi.org/10.2514/6.2018-2722

[9] Summers, Matt H., "Small-Scale Hybrid Rocket Test Stand & Characterization of Swirl Injectors," Masters Thesis, Aerospace Engineering, Arizona State University, Tempe, Arizona, 2013.

[10] Utley, Lucas J., Foster, Garett C., Rouser, Kurt P., "Design and Evaluation of a Portable, Flexible-Use Rocket Thrust Stand," *Oklahoma State University*, Stillwater, Oklahoma, 2018.

[11] Freeman, Chuck W., II, "Solid Rocket Motor Static Fire Test Stand Optimization: Load Cell Effects and Other Uncertainties," The University of Alabama in Huntsville, ProQuest Dissertations Publishing, 2018.